Pergamon

SCIENCE DIRECT®

Bioorganic & Medicinal Chemistry 11 (2003) 4207–4216

BIOORGANIC & MEDICINAL CHEMISTRY

QSAR Study of Dual Cyclooxygenase and 5-Lipoxygenase Inhibitors 2,6-di-*tert*-Butylphenol Derivatives

Juan Ruiz,* Carmen Pérez and Ramon Pouplana

Departament de Fisicoquímica, Facultat de Farmàcia, Universitat de Barcelona, Avda Joan XXIII s/n, 08028 Barcelona, Spain

Received 4 April 2003; accepted 2 July 2003

Abstract—The dual or selective ability of 24 derived mono- and 2,6-di-*tert*-butylphenols (DTBP) to act as inhibitors of cyclooxygenase (COX) and/or 5-lipoxygenase (LOX) enzymes is investigated. Firstly, we explored the conformational variability of the compounds. It is found that dual inhibitors can adopt four minimum energy conformations: *cis* or *trans*, depending on the orientation of the carbonyl oxygen atom (localized in the *para* position) relative to the hydroxyl hydrogen, and α or β, depending on whether the carbonyl oxygen is below or above the phenyl plane. The possible bioactive conformations are selected by molecular superimposition to the optimised structure of tebufelone, a dual inhibitor in the clinical trial phase. From this selected conformation, different molecular parameters were calculated and correlated with both COX/LOX inhibitory activities. The MEP and GRID maps for different probes (hydrogen bond donor/acceptor, hydrophobic and ferric/ferrous interaction areas) are represented and discussed. The results point out the importance of the hydrogen donation and the hydrophobic properties in the COX inhibition whereas, for LOX inhibition, a redox mechanism might be involved. Finally, the predictive ability of the proposed QSAR equations is tested analysing a set of selective COX or LOX inhibitors.
© 2003 Elsevier Ltd. All rights reserved.

Introduction

2,6-di-*tert*-Butylphenols (DTBP) constitute an important group of anti-inflammatory phenolic compounds owing to their antioxidant properties, which are related to inhibition of prostaglandin and leukotriene synthesis. They have a dual activity, acting as blockers of cyclooxygenase-2 (COX) and 5-lipoxygenase (5-LOX) enzymes.[1–5] The radical scavenging activity of these anti-inflammatory antioxidant compounds has increased their potential therapeutic applications in areas such as cancer cell prevention, Alzheimer's disease and asthma, where intermediate radicals participate in the disease pathogenesis.[6–9] Due to their impact in the treatment of these diseases, new DTBP compounds have been synthesized and tested for COX/5-LOX inhibitory capacity, while trying to have low ulcerogenic potential. Some of these compounds, such as tebufelone, R-830, BF389, CI-1004[2] and S2474,[10] are now under clinical trials (see Scheme 1).

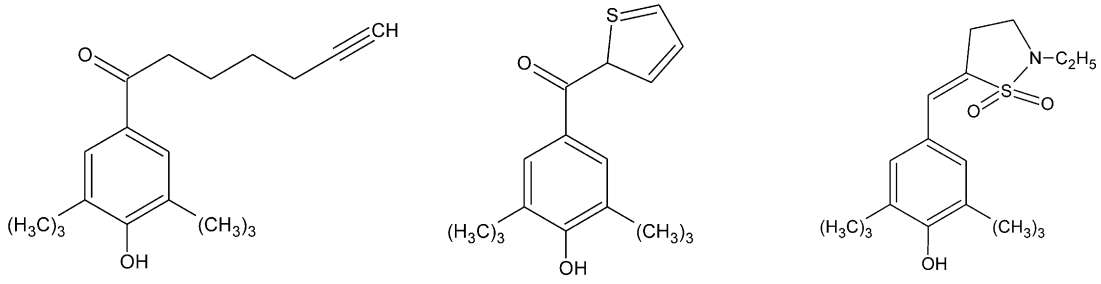

Tebufelone **R-830** **S2474**

Scheme 1. Molecular structures of DTBP used as dual inhibitors.

*Corresponding author. Tel.: +34-3-402-4557; fax: +34-3-403-5987; e-mail: juan@irene.far.ub.es

0968-0896/$ - see front matter © 2003 Elsevier Ltd. All rights reserved.
doi:10.1016/S0968-0896(03)00449-8

Mechanistic studies have addressed the relationship between the phenolic antioxidant properties and the abstraction of phenolic hydrogen, often leading to QSAR models that relate radical formation and anti-inflammatory or antioxidant activities.[11–14] In the present work, we relate the conformational variability and the calculated parameters derived from the proposed bioactive conformation with the inhibitory properties of DTBP.[1]

Material and Methods

Compounds and biological data

The general structure of the studied compounds is shown in Table 1. The major structural diversity stems from the *para* substituent (R_3 group), since *tert*-butyl groups exist at *ortho* positions (R_1 and R_2) and are necessary for an optimal antioxidant capacity by hydrogen donation.[12] However, to examine the effect of these groups, four compounds mono or unsubstituted *tert*-butyl (or methyl) fragments (compounds **11**–**14**) were also considered.

Table 1 also summarizes the dual COX/5-LOX activities of the compounds. The activities were taken from the studies of Swingle et al.[1] and are related to the estimated concentration producing 50% inhibition of bovine seminal vesicle cyclooxygenase and 50% inhibition of guinea pig lung 5-lipoxygenase (IC_{50}). To validate the proposed QSAR models and to explain the dual activity, a complementary set of 10 compounds, divided into five COX selective and five LOX selective compounds (Table 2), was also examined.

Computational methods

The initial geometries were built up from molecular mechanics (MM) calculations implemented in the Insight II program [15] on a Silicon Graphics workstation. The conformational study was carried out using the semi-empirical AM1 method using the MOPAC 6.0 ESP program [16]. Full geometry optimization of minimum energy conformations was subsequently carried out at the HF/6-31G(d) ab initio level using GAUSSIAN-94 program.[17] In order to select the possible active conformation, we superimposed the minimum energy conformations with the optimized conformations of the active dual inhibitor tebufelone (Scheme 1). The topological electron density at the O–H bond was determined using the OUTPUT = WFN option of GAUSSIAN-94 and EXTREME[18] programs.

Attention was paid to the bond critical point (ρOH), that is, the point of minimum charge density along the bond path that links two atoms, but a maximum along the directions normal to the bond path.[19] The hydrophobic contribution was evaluated from the ClogP parameter.[20]

Molecular electrostatic potential maps (MEP) were drawn using the MEPMIN program.[21] Favourable interaction areas for the selected conformation for each compound were represented using the GRID program[22,23] with the probes methyl, water, ferrous and ferric iron cations. These latter probes are important to analyze a possible redox inhibition mechanism of DTBP.[24,25]

Results and Discussion

Conformational analysis

Depending on the *para* substituent (R_3), mono or DTBP compounds show possible coplanar regions in agreement with the available crystallographic data. Compounds having an aromatic ring in R_3 have two coplanar regions in their molecular structure: (a) the coplanar arrangement of the hydroxyl group with the main phenol ring, and (b) the R_3 aromatic ring (phenyl or thienyl) linked by carbonyl, oxy or amino substituents. On the other hand, compounds with nitro, metoxy, hydroxy, or carboxy R_3 groups have one common planar disposition of these substituents with the phenol ring.

The rotation of R_3 group around the coplanar arrangement of the phenol ring was studied by means of the torsion angle α, which was rotated from 0° to 355° at intervals of 5°. The conformational energy surfaces for some representative compounds are shown in Figure 1. Full geometry optimization was subsequently carried out at the HF/6-31G(d) ab initio level for the minimum energy conformations using GAUSSIAN-94 program. The optimized structures differ about 5–15° from the AM1 minimum-energy conformations.

Acetamide in R_3 (compound **15**; Table 2) yields only two minimum energy conformations, which are shown in Figure 1a: *cis*, with the amino hydrogen in the same side of the hydroxyl hydrogen, and *trans*, with the amino hydrogen in the opposite side of the hydroxyl hydrogen. The conformational energy map shows that the two conformations are energetically similar (the enthalpies of formation differs by 0.5 kcal/mol) and result from the π–π conjugation process of the nitrogen lone pair with the aromatic system. Due this pyramidalization effect of amine nitrogen, the N–H bond presents in both conformations an almost planar disposition with the phenol ring. Similar results were found in conformational study of anti-inflammatory fenamates.[26]

Other compounds with R_3 fragments such as CO-phenyl or CO-thienyl exhibit four minimum energy conformations: two *cis* conformations, one *cis*-β with the carbonyl oxygen above the phenol plane and the other *cis*-α with the carbonyl oxygen below the phenol plane. These four conformations are shown in Figure 1b for *N*-methylamide compound **6** (R_3 = CO–NH–CH_3). Interestingly, this compound is a more active COX and LOX inhibitor than compound **15**, which appears only selective as COX inhibitor exhibiting a poor activity.

Table 1.

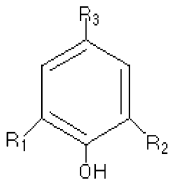

Compd	R_1	R_2	R_3	IC_{50} (μM)		ΔH_r	ρOH	ClogP	EHOMO	ELUMO	Q_{ox}	Qt	DRY	Fe2+	Fe3+
				COX[a]	5-LOX[b]										
1	$C(CH_3)_3$	$C(CH_3)_3$	CO-phenyl	9×10^{-7}	9×10^{-7}	359.4374	0.37400	6.706	−0.2907	0.1116	−0.630	−0.672	−2.222	−17.647	−23.208
2	$C(CH_3)_3$	$C(CH_3)_3$	O-phenyl	1×10^{-6}	5×10^{-7}	359.5629	0.37585	7.225	−0.2796	0.1290	−0.643	−0.136	−2.271	−20.070	−27.600
3	$C(CH_3)_3$	$C(CH_3)_3$	Phenyl	7×10^{-7}	2×10^{-7}	359.3747	0.37298	7.015	−0.2756	0.1263	−0.627	−0.489	−2.180	−20.691	−28.699
4	$C(CH_3)_3$	$C(CH_3)_3$	CO-2-thienyl (R830)	5×10^{-7}	2×10^{-5}	359.7512	0.37387	6.429	−0.3186	0.0626	−0.607	−0.534	−2.512	−11.757	−13.818
5	$C(CH_3)_3$	$C(CH_3)_3$	CO-5CI-2-thienyl	1×10^{-6}	2×10^{-6}	359.8140	0.37366	6.923	−0.3138	0.0654	−0.621	−0.593	−2.633	−15.237	−20.335
6	$C(CH_3)_3$	$C(CH_3)_3$	CO-NH-CH_3	2×10^{-6}	2×10^{-6}	360.0022	0.37456	3.861	−0.3080	0.1244	−0.630	−0.937	−2.445	−18.010	−24.314
7	$C(CH_3)_3$	$C(CH_3)_3$	NO_2	1×10^{-4}	1×10^{-4}	360.1277	0.37277	1.835	−0.3316	0.0750	−0.590	−0.105	−2.269	−8.635	−9.808
8	$C(CH_3)_3$	$C(CH_3)_3$	OH	1×10^{-4}	5×10^{-5}	360.1904	0.36745	3.460	−0.3046	0.1117	−0.612	−0.015	−1.942	−10.242	−15.303
9	$C(CH_3)_3$	$C(CH_3)_3$	COOH	1×10^{-4}	1×10^{-4}	360.3159	0.36847	3.609	−0.3188	0.0939	−0.568	−0.106	−2.134	−10.941	−12.741
10	$C(CH_3)_3$	$C(CH_3)_3$	O–CH_3	5×10^{-5}	1×10^{-4}	360.2532	0.36744	4.226	−0.3180	0.0926	−0.589	−0.011	−2.010	−12.453	−14.395
11	$C(CH_3)_3$	H	$O(CH_3)_3$ (BHA)	7×10^{-6}	1×10^{-6}	360.8180	0.36754	3.400	−0.2839	0.1438	−0.633	+0.037	−1.981	−13.064	−19.371
12	$C(CH_3)_3$	H	Phenyl	1×10^{-6}	8×10^{-7}	360.8807	0.36714	5.189	−0.2850	0.1247	−0.614	−0.671	−2.128	−14.392	−20.096
13	CH_3	CH_3	CO-phenyl	1×10^{-4}	2×10^{-5}	360.5042	0.36798	4.052	−0.3108	0.0907	−0.578	+0.230	−2.225	−10.007	−12.276
14	H	H	CO-phenyl	1×10^{-5}	1×10^{-4}	360.4414	0.36628	3.054	−0.3310	0.0884	−0.598	−1.037	−2.403	−4.297	−5.551

ΔH_r, reaction energy in kcal/mol for phenoxyl radical formation; ρOH, electron density at the O–H bond critical point; Q_{ox}, atomic charge of phenolic oxigen; *Qt*, Sum of atomic charges of *ortho* and *para* carbons of phenol ring Σ(qo + qp); DRY, minimum GRID energy interaction for hydrophobic probe; Fe2+ and Fe3+, minimum energy interaction values for ferrous and ferric iron cation probes.

[a]Micromolar concentration producing 50% inhibition of bovine seminal vesicle cyclooxygenase.

[b]Micromolecular concentration producing 50% inhibition of guinea pig lung 5-lipoxygenase.

Table 2.

Selective COX	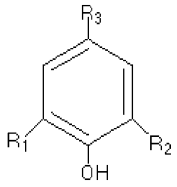					COX IC_{50} (μM)		
							Eq 5	
Compd	R_1	R_2	R_3	Qt	ClogP	Obs	Calcd	% Dev
15	$C(CH_3)_3$	$C(CH_3)_3$	NH–CO–CH_3	+0.002	3.496	4.301	4.316	0.35
16	$C(CH_3)_3$	$C(CH_3)_3$	NH-phenyl	−0.004	6.305	4.301	4.681	8.83
17	$C(CH_3)_3$	H	CO-phenyl	−0.944	4.880	6.699	6.550	−2.23
18	*i*-C_3H_7	H	CO-phenyl	−0.955	4.880	5.222	5.210	−0.23
19	$C(CH_3)_3$	H	CO-2-thienyl	−0.921	4.771	7.000	6.483	−7.38
Selective LOX						LOX IC_{50} (μM)		
							Eq 7	
Compd	R_1	R_2	R_3		Fe3+	Obs	Calcd	% Dev
20	$C(CH_3)_3$	$C(CH_3)_3$	CH_3 BHT		−23.24	6.097	6.151	0.88
21	$C(CH_3)_3$	$C(CH_3)_3$	CH_2-phenyl		−25.14	6.155	6.058	−1.57
22	$C(CH_3)_3$	$C(CH_3)_3$	CO-2-pyridyl		−21.82	5.301	5.287	−0.26
23	$C(CH_3)_3$	$C(CH_3)_3$	CO-4-pyridyl		−28.82	7.000	6.895	−1.51
24	$C(CH_3)_3$	CH_3	CO-phenyl		−13.59	5.097	4.915	−3.57

The preceding results suggests that molecular flexibility can be relevant in the modulation of the COX inhibitory activity. A similar finding can be deduced for the selective LOX inhibitors, as derived from the conformational analysis of R_3 pyridyl compounds **22** and **23**. The R_3 = CO-2-pyridyl derivative (**22**) has only two minimum energy conformations *cis* and *trans* (see Fig. 2). In contrast, the R_3 = CO-4-pyridyl analogue (**23**) is conformationally more flexible, being able to adopt four minimum energy conformations: *cis*-α, *cis*-β, *trans*-α and *trans*-β. The difference in conformational flexibility could explain, at least in part, the larger inhibitory activity of compound **23** ($IC_{50} = 1 \times 10^{-7}$ M) compared to compound **22** ($IC_{50} = 5 \times 10^{-6}$ M).

Other compounds, like the R_3 benzyl (compound **21**; see Fig. 1c), presents six minimum energy conformations: *cis*-α, *cis*-β, *trans*-α, *trans*-β, and two extra conformations, α and β, having the benzyl group in a central disposition with respect to the hydroxyl group, but below (α) or above (β) the phenol plane (Fig. 1c). The energy barrier between these conformations is, nevertheless, very low (less than 1 kcal/mol).

To select the bioactive conformation, all minimum energy conformations of the most active COX and LOX inhibitors were compared by means a superimposition procedure showing a correct fit for all four conformations (*cis*-α, *cis*-β, *trans*-α, *trans*-β) between 0.010 and 0.015; in this way, Figure 3a shows as example the superimposition of active DTBP compounds in *cis*-β conformation indicating a common binding structure with the COX and/or LOX enzymes. These superimpositions were compared with the active dual compound tebufelone obtaining also a correct fit depicted in Figure 3b for compound **1** in the *cis*-β conformation (RMS = 0.031).

QSAR analysis

A series of recent studies have shown the relevance of electronic properties in modulating the anti-inflammatory antioxidant activity of phenols.[10–12] Our previous works[13,14] allowed us to find a significant correlation between the enthalpy of the phenoxyl radical formation process and the COX inhibitory activity of phenols.

For the series of DTBP compounds, the enthalpy of reaction (ΔH_r) of radical formation, defined as the difference between the enthalpies of ground and radical states, were also calculated. The ΔH_r values (see Table 1) are quite similar in all compounds and no significant relationships were obtained between the ΔH_r values and the COX or LOX inhibitory activity, which was unexpected based on the correlations between ΔH_r and OH bond dissociation energies reported for phenolic compounds.[27,28] However, the most active DTBP compounds (**1**–**5**) have ΔH_r values 1 kcal/mol lower than the rest of compounds (see Table 1), a finding also found in QSAR studies of phenols.[14]

Due to the importance of electronic parameters in QSAR studies of anti-inflammatory-antioxidants inhibitors,[11–14] the electron density at bond critical point (ρOH) was also determined, since it can be used as a predictor of hydrogen-bond donation.[10–12] Table 1 summarizes the calculated ρOH for DTBP compounds. The most active inhibitors have a high electron density at the OH bond, while the less active inhibitors tend to have a low electron density at the OH bond. Interestingly, mono-*tert*-butyl-phenols present lower ρOH values, as expected from the lack of one electron-donating substituent, thus reducing the DTBP-phenoxyl radical formation. Not unexpectedly, there is a clear correlation between the capacity to form the phenoxyl

radical (ΔH_r) and the electron density at the OH bond (ρOH), as noted in eq 1.

$$\Delta H_r = -113.91(\pm 22.16)\rho OH + 402.33(\pm 8.21) \quad (1)$$

$$n = 14 \;\; r^2 = 0.688 \;\; Q^2 = 0.587 \;\; s = 0.202 \;\; F = 26.42$$

Other parameters, such as the atomic charges and the energies of the highest-occupied (EHOMO) and lowest-unoccupied molecular (ELUMO) orbital, were also considered. Table 1 summarizes the results of these electronic parameters for the *cis*-β conformation. Their analysis showed that EHOMO correlates with LOX inhibitory activity ($r^2 = 0.784$; eq 2). No correlation was found between EHOMO and COX inhibitory activity. Similarly, ELUMO was unable to explain the differences in COX/LOX inhibitory activity.

$$pIC_{50}(LOX) = 47.25(\pm 7.21)EHOMO + 19.57(\pm 2.20) \quad (2)$$

$$n = 14 \;\; r^2 = 0.784 \;\; Q^2 = 0.695 \;\; s = 0.489 \;\; F = 42.88$$

The atomic charge of hydroxyl oxygen (Q_{ox}) correlates with the two activities (COX, $r^2 = 0.567$; LOX,

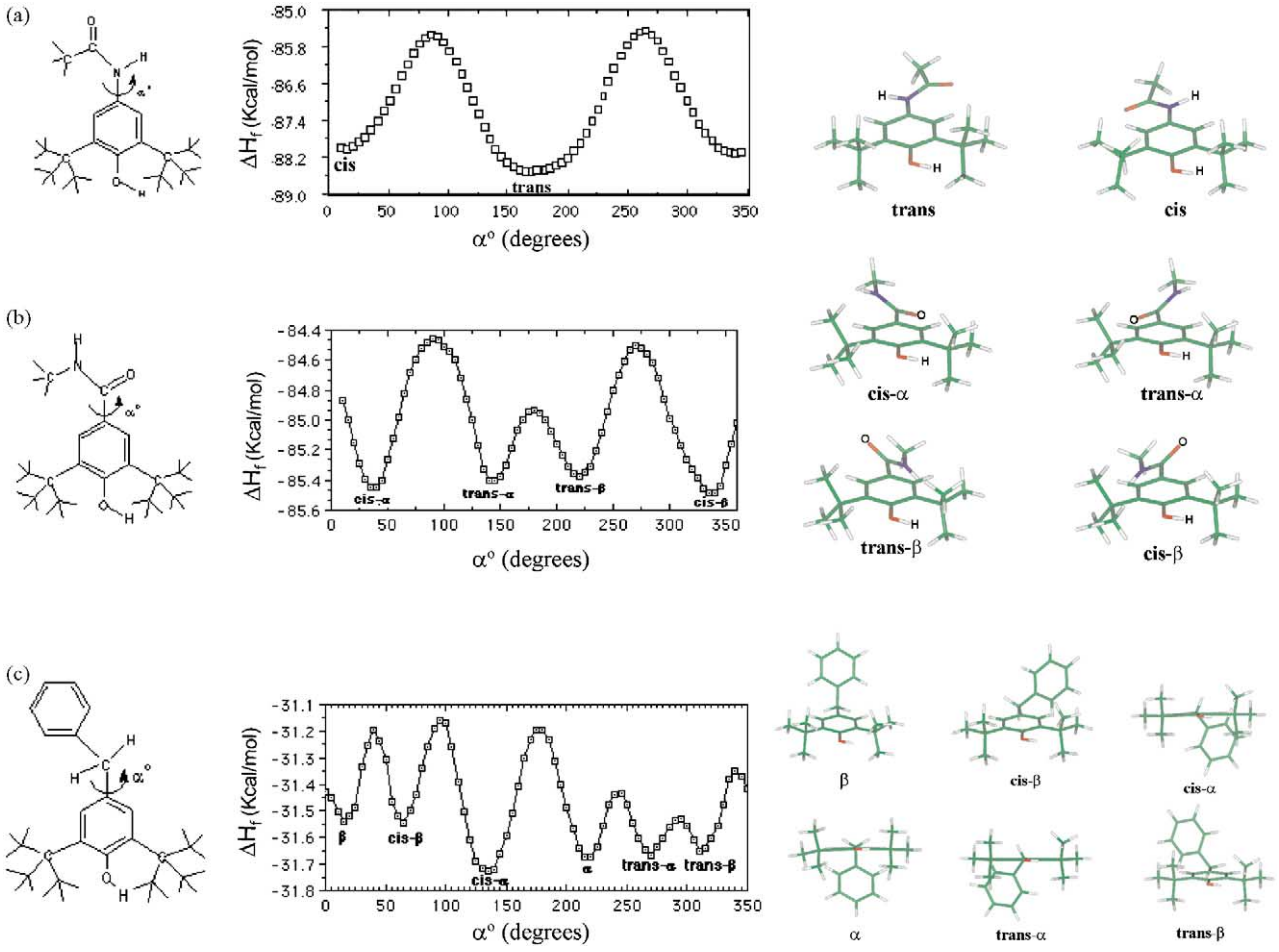

Figure 1. Conformational energy surfaces and minimum energy conformations for: (a) the selective COX inhibitor **15**, (b) the dual compound **6** and (c) the R_3 benzyl compound **21**.

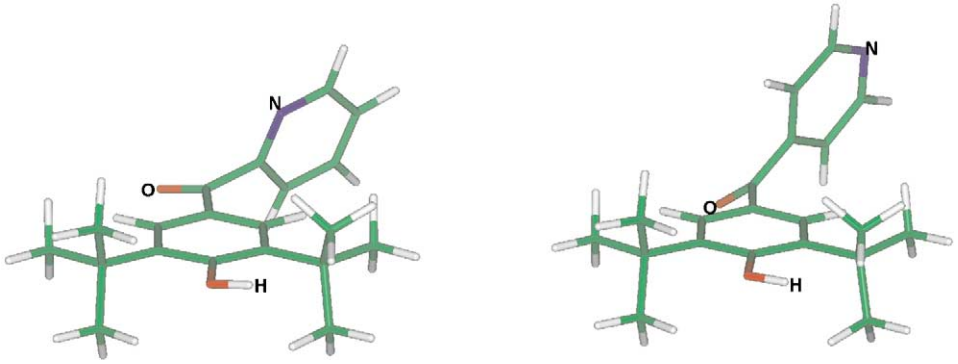

Figure 2. Comparison of the *trans*-α minimum-energy conformations of 2-pyridyl and 4-pyridyl-DTBP (**22** and **23**) compounds.

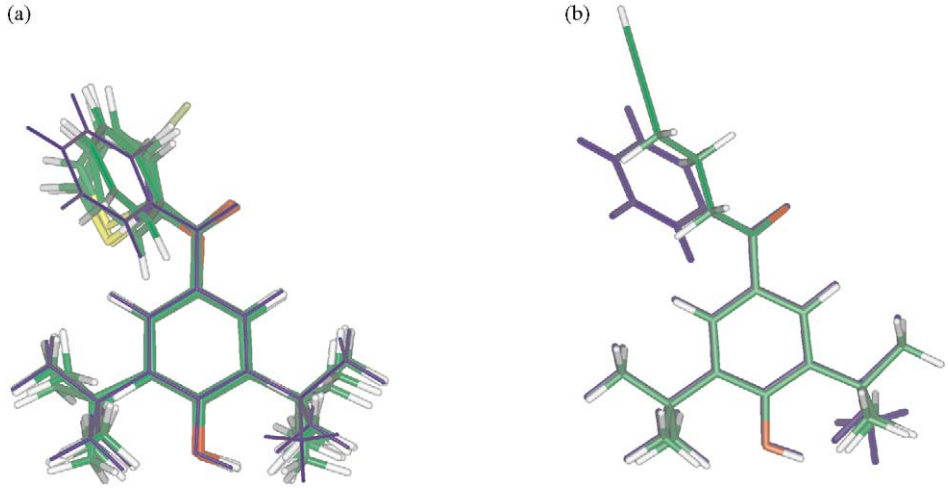

Figure 3. (a) Superimposition for the *cis*-β minimum-energy conformation of different DTBP compounds; (b) superimposition of the *cis*-β conformations of the active dual *p*-benzoyl-DTBP (**1**) and tebufelone.

$r^2 = 0.693$, eq 3). The regression equations indicate that the more negative Q_{ox}, the larger the inhibitory activity. Thus, the larger activity of compounds **1**–**3** compared to that of compounds **7**–**9** can be related to the *para* substitution with electron-withdrawing substituents (carboxyl, nitro, or hydroxyl) for these latter molecules. Moreover, the lack of the two electron-donating (*tert*-butyl) groups at *ortho* position makes Q_{ox} to be less negative, thus reducing the inhibitory activity (compounds **13** and **14**).

$$pIC_{50}(LOX) = -37.09(\pm 7.13)Q_{ox} - 17.47(\pm 4.35) \quad (3)$$

$$n = 14 \;\; r^2 = 0.693 \;\; Q^2 = 0.626 \;\; s = 0.589 \;\; F = 27.08$$

The atomic charges at *ortho* and *para* carbons were also examined, but no correlation was found with the inhibitory activity. However, attachment of *tert*-butyl groups at *ortho* positions decrease the negative atomic charge as follows: di-*tert*-butyl (**1**) < mono-*tert*-butyl (**17**) < unsubstituted (**14**) ($-0.512 < -0.726 < -0.852$). A similar effect is obtained considering the sum of atomic charges of carbon atoms at *ortho* and *para* positions (Qt) [$-0.672 < -0.944 < -1.037$].

To investigate the role of hydrophobicity, the ClogP parameter[20] was determined (see Table 1). The *tert*-butyl fragments increase the ClogP from 3.054 (**14**) to 4.880 (**17**) to 6.706 (**1**). In contrast, the less active compounds posses an hydrophilic fragment in the phenol ring, such as nitro (**7**), hydroxy (**8**) or carboxy (**9**), thus reducing the ClogP. These results reinforce previous QSAR studies about anti-inflammatory inhibitors, where a high ClogP was found to increase the inhibitory potency. For DTBP compounds, the ClogP yielded a better correlation with COX inhibitory activity ($r^2 = 0.645$, eq 4) than with LOX ($r^2 = 0.371$).

$$pIC_{50}(COX) = 0.43(\pm 0.09)ClogP + 3.13(\pm 0.47) \quad (4)$$

$$n = 14 \;\; r^2 = 0.645 \;\; Q^2 = 0.566 \;\; s = 0.586 \;\; F = 21.78$$

The combination of ClogP with the previous electronic parameters improves the correlation equations for both COX and LOX activities, as can be seen in eqs 5 and 6.

$$pIC_{50}(COX) = -1.11(\pm 0.29)Qt + 0.37(\pm 0.07)ClogP + 3.02(\pm 0.32) \quad (5)$$

$$n = 14 \;\; r^2 = 0.845 \;\; Q^2 = 0.767 \;\; s = 0.405 \;\; F = 29.81$$

$$pIC_{50}(LOX) = 38.82(\pm 8.01)EHOMO + 0.16(\pm 0.08)ClogP + 16.25(\pm 2.70) \quad (6)$$

$$n = 14 \;\; r^2 = 0.833 \;\; Q^2 = 0.745 \;\; s = 0.440 \;\; F = 27.46$$

Molecular electrostatic potential (MEP) maps

To explore the interaction capabilities of DTBP, the MEP was determined for the series of compounds in their minimum-energy conformations. Figure 4 compares the MEP map distribution for some representative compounds in the optimized *cis*-β conformation. In general, the MEP maps show four minima: the first placed in the hydroxyl group, the second and third at each side of the phenyl ring, and the fourth near the carbonyl group. These minima occur in selective COX inhibitors (see Fig. 4a for compound **15**). On the other hand, selective LOX and dual inhibitors present an additional extended negative region around the R3 aromatic ring group, as shown in Figure 4b for the LOX inhibitor **23** and Figure 4c for the dual compound **3**. The less active compounds, such as **8** (see Fig. 4d), have a different pattern of MEP minima.

GRID maps

GRID was used to identify possible areas of interaction with selected probes: hydrophobic (DRY), water (OH2), ferric and ferrous iron cation (Fe^{3+} and Fe^{2+}).

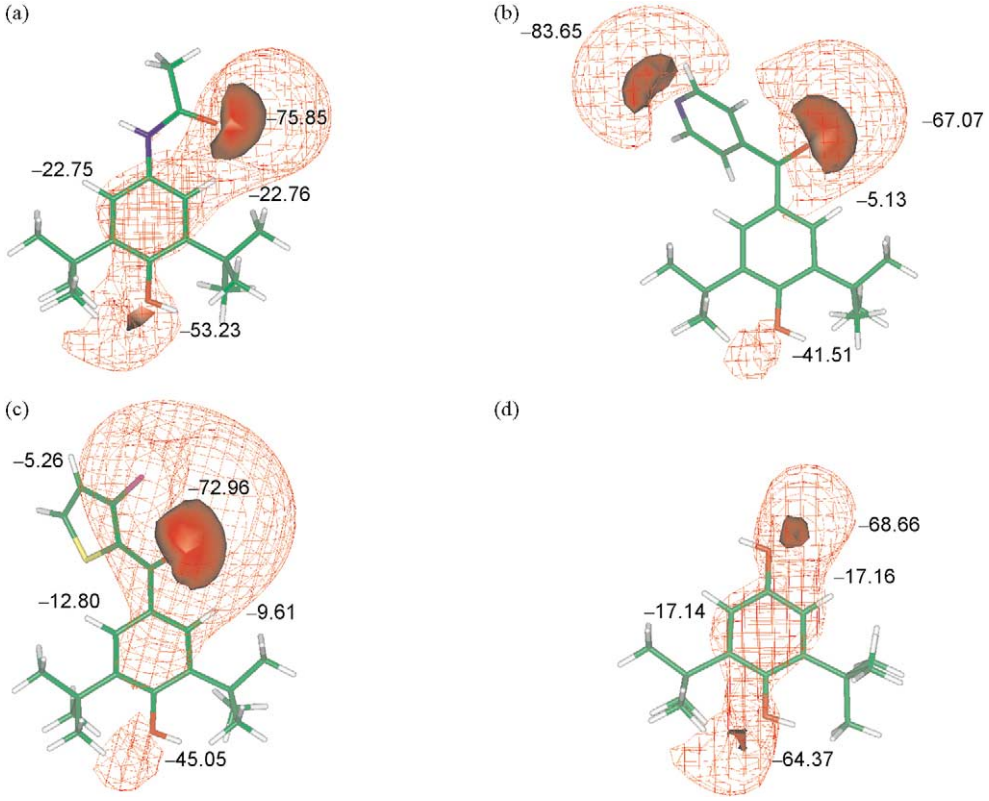

Figure 4. MEP maps for the minimum energy *cis*-β conformation of: (a) the selective COX inhibitor **15**, (b) the selective LOX inhibitor **23**, (c) the dual compound **5** and (d) the less active compound **8**. Dotted red lines correspond to an isocontour energy level of −10 kcal/mol and solid red contours to −50 kcal/mol.

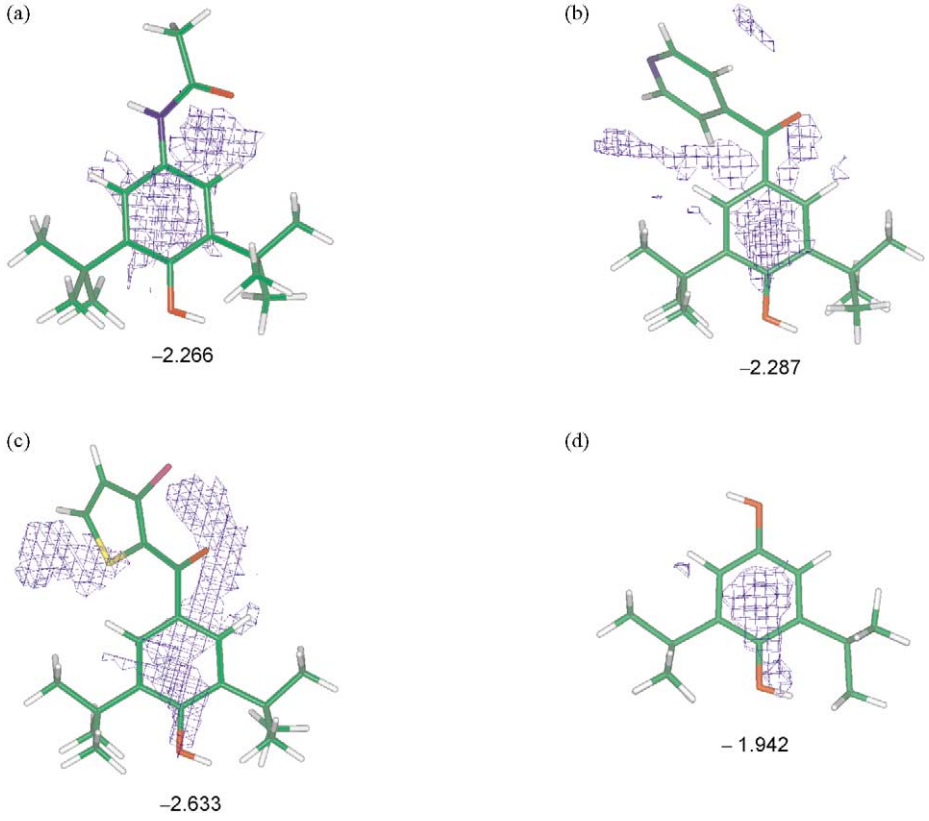

Figure 5. GRID hydrophobic (DRY) probe maps for different DTBP compounds in *cis*-β conformation. The contour level corresponds to −1.5 kcal/mol and the maximum interaction energy value is indicated below each molecule: (a) the selective COX inhibitor **15**, (b) the selective LOX inhibitor **23**, (c) the dual active compound **5** and (d) the less active compound **8**.

Comparison of the interaction areas for the DRY hydrophobic probe for four representative compounds is given in Figure 5. For each compound the most favourable interaction energy is placed around the phenol ring. Selective COX inhibitors present another complementary area (Fig. 5a) near the R_3 substituent, whereas for selective LOX inhibitors (Fig. 5b) this area is around the second aromatic ring and dual inhibitors (Fig. 5c) exhibit both areas. In contrast, the less active compound **8** (Fig. 5d) has a reduced area for hydrophobic interaction and a less favourable interaction energy (−1.9 kcal/mol) compared to the active compounds.

The water probe (OH2) allows us to explore potential areas for hydrogen bond donor and acceptor contacts.[29] There are two common areas for all compounds: one around the hydroxyl group and another around the *para* carbonyl group. These areas for the dual active BHA (compound **11**) and the less active compound **10** are shown in Figure 6, which indicates that they are larger around the hydroxyl group for the BHA compound.

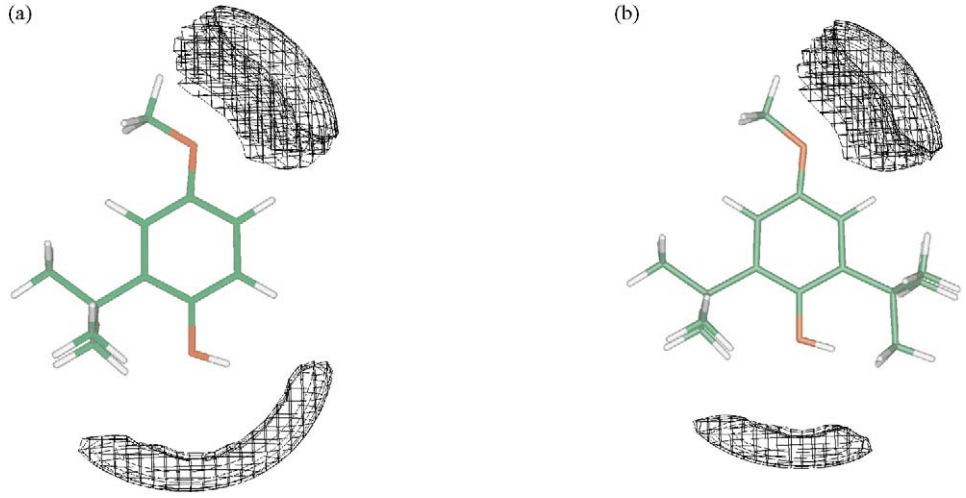

Figure 6. Possible hydrogen-bond acceptor and donor regions derived from GRID maps for the water (OH2 probe) for: (a) the active dual BHA compound **11** and (b) the less active compound **10**. This latter compound shows a more reduced area for the hydrogen-bond donor region placed at the hydroxyl group.

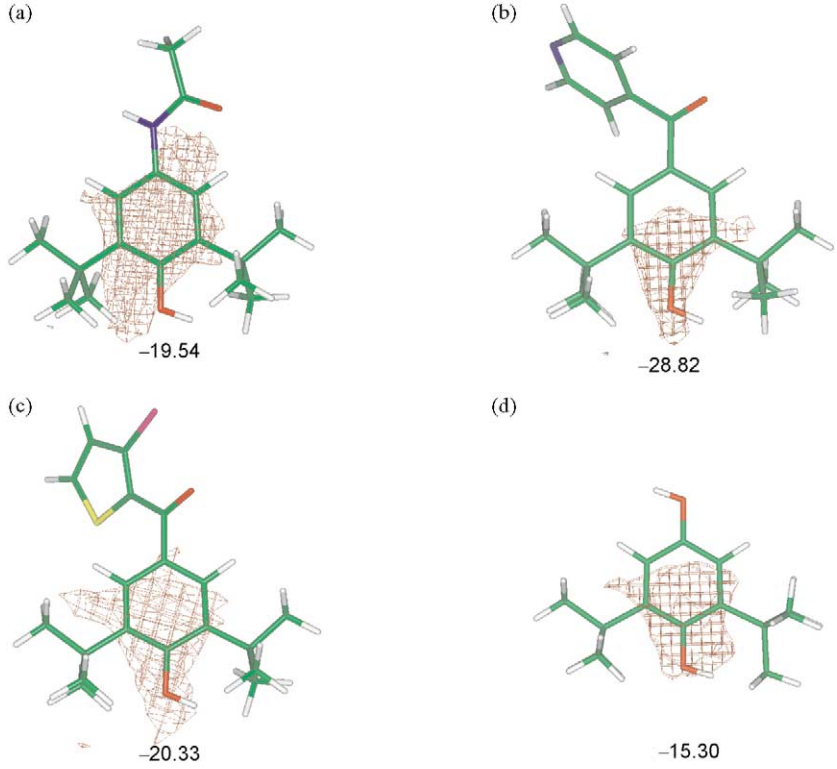

Figure 7. GRID interaction for ferric iron cation probe for different DTBP compounds. The contour level corresponds to −10 kcal/mol and the maximum interaction energy value is indicated below each molecule: (a) the selective COX inhibitor **15**, (b) the selective LOX inhibitor **23**, (c) the dual active compound **5** and (d) the less active compound **8**.

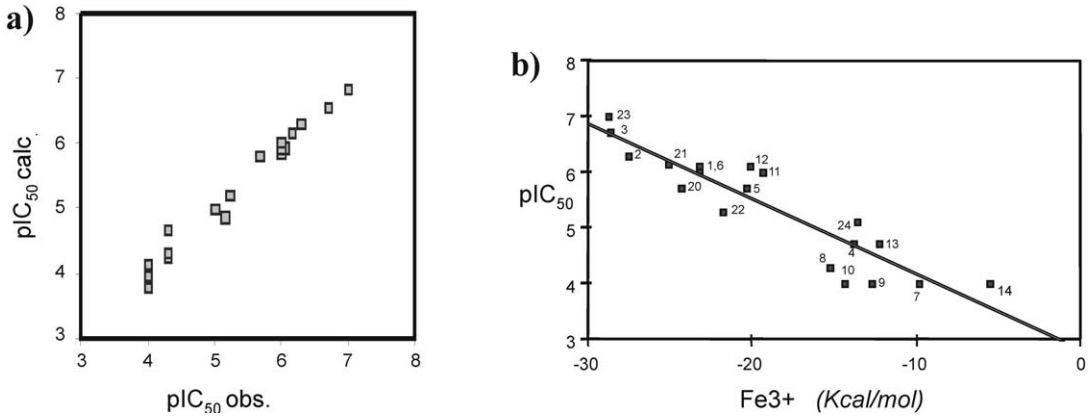

Figure 8. Linear regression of observed: (a) cyclooxygenase inhibitory activity pIC_{50} versus the calculated from eq 5, (b) lipoxygenase inhibitory activity with the ferric iron cation (Fe3+) minimum energy of interaction from eq 7.

Finally, Figure 7 shows the Fe3+ GRID maps for selected DTBP compounds in *cis*-β conformation. The two probes for Fe interaction yield similar maps for all the compounds, leading to a main interaction area proximal to the phenol ring that involves the hydroxyl fragment. Active LOX inhibitors have higher interaction energy than COX inhibitors. Thus, tebufelone presents a Fe3+ interaction energy around 22 kcal/mol more negative than the less active compounds (−15.30 kcal/mol for compound **8**; Fig. 7d). Because of the common interaction pattern for all the compounds, we correlated these values with the activities. It was found that Fe3+ correlates better than Fe2+ and preferably with LOX ($r^2 = 0.823$, eq 7) than COX ($r^2 = 0.452$) inhibitory activity.

$$pIC_{50}(LOX) = -0.13(\pm 0.02)Fe3^{+} + 2.79(\pm 0.34) \qquad (7)$$

$$n = 14 \;\; r^2 = 0.823 \;\; Q^2 = 0.792 \;\; s = 0.440 \;\; F = 55.88$$

This finding is in agreement with eq 2, where EHOMO expresses the electron-donor capacity as the energy required to remove the most external electron. In fact, both Fe3+ interaction energies and EHOMO are highly correlated, as noted in eq 8, indicating that compounds with a high EHOMO have a low energy for Fe3+ interaction.

$$EHOMO = -0.002(\pm 0.00)Fe3 + -0.35(\pm 0.01) \qquad (8)$$

$$n = 14 \;\; r^2 = 0.719 \;\; Q^2 = 0.639 \;\; s = 0.010 \;\; F = 30.63$$

Finally, to evaluate the predictive capability of eqs 5 and 7, five selective COX and five selective LOX inhibitors were additionally examined. The results are given in Table 2. The calculated activities shows a correct fit ranging from −7.38 to 8.83% from the experimental pIC_{50} COX activity and between −3.57 and 1% from pIC_{50} LOX activity [see Fig. 8a ($n = 19$, $r^2 = 0.978$) and b ($n = 19$, $r^2 = 0.837$)].

Conclusions

For the series of DTBP derivatives, the conformational analysis indicates that they can adopt four common minimum energy conformations (*cis*-α, *cis*-β, *trans*-α, *trans*-β) that shows a correct fit with the structure of the dual activity compound tebufelone. With exception of the classical antioxidant BHA (compd **11**), for a high dual activity the optimal structure is to present two aromatic rings, which permits a major conformational variability and perhaps a more effective interaction with the COX/LOX binding site.

The analysis of QSAR parameters points out the importance of the presence of electron donating substituents as *tert*-butyl group in the *ortho* positions of the phenol ring. Their presence favors the phenoxyl radical formation (hydrogen donation) and the hydrophobic binding to COX-LOX enzymes, although the hydrophobic requirement seems more important in COX. The high negative atomic charge in the phenolic (*ortho* + *para*) ring correlates preferably with the COX inhibition, suggesting a possible complementary π–π interaction of DTBP for the COX interaction process. On the other hand, the high negative atomic charge at the oxygen atom of the hydroxyl fragment favors the hydrogen donation correlating with the activity to inhibit both enzymes.

The LOX inhibitory activity correlates with both EHOMO and Fe3+ interaction energies. The most active dual and selective LOX inhibitors present a high EHOMO and a low FE3+ interaction energies, which suggest a possible Fe-redox mechanism for LOX inhibition that could help to understand the dual inhibitory capacity of DTBP compounds. Following this hypothesis, the dual inhibitory effects could help to develop new anti-inflammatory compounds.

Acknowledgements

We thank Prof. F. J. Luque for the valuable comments and help in the preparation manuscript, Prof. R. F. W. Bader for providing his codes for the topological analysis of the electron density and Prof. David Leo for his version of the CLogP program. We also thank the Centre de Supercomputació de Catalunya (CESCA) for the computational support in ab initio calculations.

References and Notes

1. Swingle, K.F.; Bell R.L.; Moore, G.G.I. In *Anti-inflammatory and Anti-rheumatic Drugs*; Rainsford Ph. D. K. D., Path, M. R. C., Eds.; CRC: Florida, 1989; Vol. 3, p 105.
2. Dyer, R. D.; Connor, D. T. *Curr. Pharm. Des.* **1997**, *3*, 463.
3. Kramer, J. B.; Capiris, T.; Sircar, J. C.; Connor, D. T.; Bornemeier, D. A.; Dyer, R. D.; Kuipers, P. J.; Kennedy, J. A.; Wright, C. D.; Okonkwo, G. C. N.; Lesch, M. E.; Schrier, D. J.; Boschelli, D. H. *Bioorg. Med. Chem.* **1995**, *3*, 403.
4. Fiorucci, S.; Meli, R.; Bucci, M.; Cirino, G. *Biochem. Pharmacol.* **2001**, *62*, 1433.
5. Lazer, E. S.; Wong, H. C.; Possanza, G. J.; Graham, A. G.; Farina, P. R. Antiinflammatory. *J. Med. Chem.* **1989**, *32*, 100.
6. Behl, Ch.; Moosmann, B. *Free Rad. Biol. Med.* **2002**, *33*, 182.
7. Rioux, N.; Castonguay, A. *Carcinogenesis* **1998**, *19*, 1394.
8. Sugaya, K.; Uz, T.; Kumar, V.; Manev, H. *Jpn. J. Pharmacol.* **2000**, *82*, 8594.
9. Bertolini, A.; Ottani, A.; Sandrini, M. *Pharmacol. Res.* **2001**, *44*, 437.
10. Inagaki, M.; Tsuri, T.; Jyoyama, H.; Ono, T.; Yamada, K.; Kobayashi, M.; Hori, Y.; Arimura, A.; Yasui, K.; Ohno, S.; Kakudo, S.; Koizumi, K.; Suzuki, R.; Kawai, S.; Kato, M.; Matsumoto, S. *J. Med. Chem.* **2000**, *43*, 2040.
11. Lien, E. J.; Ren, S.; Bui, H. H.; Wang, R. *Free Rad. Biol. Med.* **1999**, *26*, 285.
12. Tomiyama, S.; Sakai, S.; Nishiyama, T.; Yamada, F. *Bull. Chem. Soc. Jpn.* **1993**, *66*, 299.
13. Ruiz, J.; Pérez, A.; Pouplana, R. *Quant. Struct. Act. Relat.* **1996**, *15*, 219.
14. Ruiz, J.; Pouplana, R. *Quant. Struct. Act. Relat.* **2002**, *21*, 605.
15. BIOSYM Technologies, Inc.: 10065 Barnes Canyon Road, San Diego, CA 92121, USA, 2002.
16. Kollman, P. A. *J. Comput. Chem.* **1990**, *11*, 431.
17. Frisch, M. J.; Trucks, G. W.; Schlegel, H. B.; Gill, P. M. W.; Johnson, B. G.; Robb, M. A.; Cheeseman, J. R.; Keith, T.; Petersson, G. A.; Montgomery, J. A.; Raghavachari, K.; Al-Laham, M. A.; Zakrzewski, V. G.; Ortiz, J. V.; Foresman, J. B.; Cioslowski, J.; Stefanov, B. B.; Nanayakkara, A.; Challacombe, M.; Peng, C. Y.; Ayala, P. Y.; Chen, W.; Wong, M. W.; Andres, J. L.; Replogle, E. S.; Gomperts, R.; Martin, R. L.; Fox, D. J.; Binkley, J. S.; Defrees, D. J.; Baker, J.; Stewart, J. P.; Head-Gordon, M.; González, C.; People, J. A. *GAUSSIAN 94, Rev. E.1*; Gaussian Inc.: Pittsburgh, PA, 1995.
18. Biegler-Ksning, F. W.; Bader, R. F. W.; Tang, T. H. *J. Comput. Chem.* **1982**, *3*, 317.
19. Bader, R. F. W.; Essén, H. *J. Chem. Phys.* **1984**, *80*, 1943.
20. ClogP algorithm designed by Dr. Albert Leo programmed by Dr. David Weininger Biobyte Corp. 201 W. 4th St. Suite #204 Claremont, CA 91711, USA, 1996.
21. Sanz, F.; Manaut, F.; Rodríguez, J.; Lozoya, E.; López de Briñas, E. *J. Comput. Aided Mol. Des.* **1993**, *7*, 337.
22. Goodford, P. J. *J. Med. Chem.* **1985**, *28*, 849.
23. *GRIN, GRID, GRAB and GROUP*, version 16.0; Molecular Discovery Ltd.; London, UK, 1998.
24. Skrzypczak-Jankun, E.; Funk, M. O., Jr.; Boyington, J. C.; Amzel, L. M. *J. Mol. Struct.* **1996**, *374*, 47.
25. Young, R. N. *Eur. J. Med. Chem.* **1999**, *34*, 671.
26. Lozano, J. J.; Pouplana, R.; López, M.; Ruiz, J. *J. Mol. Struct. (Theochem.)* **1995**, *335*, 215.
27. Bordwell, F. G.; Zhang, X.-M.; Satish, A. V.; Cheng, J.-P. *J. Am. Chem. Soc.* **1994**, *116*, 6605.
28. Bean, G. P. *Tetrahedron* **2002**, *58*, 9941.
29. Segarra, V.; López, M.; Ryder, H.; Palacios, J. M. *Quant. Struct. Act. Relat.* **1999**, *18*, 474.